

Multiple-input multiple output wireless systems - a geometrical explanation of how they work

Peter F. Driessen

Electrical and Computer Engineering, University of Victoria
Victoria, B.C., Canada, driessen@uvic.ca, www.peterx.com

Abstract— For fixed bandwidth and total radiated power, with Rayleigh fading, a wireless system with multiple antennas at both transmitter and receiver has a channel capacity which grows linearly (rather than logarithmically) with the number of antennas. This result, which assumes separate information is sent out of each transmit antenna, holds true even though the transmitter does not know the complex channel transfer characteristic. By explicitly spreading out the antennas well beyond a wavelength, we show that such capacities can be achieved not only on Rayleigh channels with many scatterers, but also on deterministic channels with direct line-of-sight (LOS) paths only and no scatterers. Roughly speaking, the wide spacing, replicates the effect of scatterers which create images and thus serves to spread out the apparent source of the signals over a wider angular range. In this way capacities on the order of $C_{lin} = n \log_2(1 + \rho)$ bps/Hz can be obtained for LOS as well as Rayleigh channels when n transmit and n receive antennas are used. In contrast, when the transmit antennas are closely spaced, the number of degrees of freedom on a LOS channel degenerate, resulting in capacities of only $C_{log} = \log_2(1 + n\rho)$.

I. INTRODUCTION

As previously reported [1], wireless communications channels with multiple antennas at both transmitter and receiver have an information-theoretic capacity which can grow linearly (rather than logarithmically) with the number of antennas, for fixed power and bandwidth. Such linear growth is found when the matrix channel transfer function between the transmitter and receiver antennas is modelled statistically, as a matrix with independent complex gaussian (scalar) random variable entries (to represent Rayleigh fading), so that then capacity is expressed as a random variable. At a specified outage level, the capacity is increased in direct proportion to the number of degrees of freedom [1].

In a Rayleigh fading environment, with scattered signals arriving from many directions, and n antennas at each site, n degrees of freedom are possible [1], assuming an antenna spacing of about half-wavelength for which mutual coupling effects are negligible. However, in certain propagation environments, particularly when there is a deterministic or line-of-sight (LOS) component, the number of degrees of freedom can degenerate [1]. For example, with n -level receive diversity of the maximum ratio combining type, which is a well known form of diversity, the capacity increases only logarithmically with n . The increase is due only to the SNR gain from the array of the n receive antennas.

The question arises as to whether it is possible to retain

the linear capacity growth with n for channels with a significant deterministic component. Thus this paper explores the capacities which may be achieved in propagation environments where there is a strong deterministic component adding to the statistical character of the matrix channel. We will parametrize channel characteristics so we can analyze the range from Rayleigh to Rician to purely LOS channels.

A. Capacity as a random variable

As discussed in [1], the sort of channel under study here is an idealization of the kind of channel occurring in, for example, burst communication mobile wireless applications. The capacity increases that we uncover are aimed at improving deliverable bit rates in such situations. Indoor wireless applications [1][2] represent another important realm of potential application for the results presented here. The results also apply to outdoor mobile channels.

Even though the base and user in an office LAN environment may involve very small mobility, we treat capacity as a random variable. Another example where we treat capacity as random involves when transmit and receive sites are secured say to buildings. In both these application areas the seeming immobility of such channels is only nominal as there can be small (and large) perturbations of the propagation environments as well as the communication sites. For indoor LANs the users may move somewhat about the workspace. There can also be significant movement of workers, equipment, file cabinets, metal doors, mail carts, elevators etc. For predominately outdoor inter-building links there are thermal and wind stresses of antenna structures as well as significant channel changes due to for example vehicle and foliage movement. As we will see, half-wavelength movement can be highly significant. We idealize here and take the view that the channel changes have a slow time constant relative to the duration of a communication burst. We allow that from burst to burst the channel may vary and one might be interested in the capacity that can be attained in nearly all (e.g. 99 percent) of the transmissions¹. For this reason we will highlight complementary capacity distributions with special attention to the high probability (small outage) tail. The complementary one percent of the situations when a

¹However, it is worth reiterating [1] that in some special applications, like very large file transfers, maximum throughput possible over long time periods may be a more relevant criterion than the 99-percentile capacity.

desired capacity level cannot be obtained is termed channel outage.

We emphasize that the information-theoretic capacity is an ultimate limit to capacity, and in practice can only be approached. So here capacity simply serves as a performance indicator: In applications one can only strive to get some fraction of capacity at an acceptably low bit-rate. It is important keep the distinction between outage (times when the channel is fundamentally inadequate) and required bit-error rate (errors due to noise when the channel is adequate). In many applications the latter is orders of magnitude more stringent than one percent (.01).

B. Ray tracing for the deterministic component of capacity

Our investigations use ray tracing to construct an $n \times n$ matrix channel response explicitly for a specified environment with obstructions and scatterers, including smooth walls as well as rough surfaces [7]. Such a channel response will change as the receiver is moved, so that a capacity distribution is obtained from the ensemble of sample matrix elements at different receiver locations. Alternatively, a deterministic matrix may be added to the Rayleigh matrix to form a matrix of Ricean scalars, from which a capacity distribution is obtained. As part of this study, we will find the capacities which may be achieved for particular realizations of the channel matrix (i.e. one sample of the ensemble of sample matrix elements), and show explicitly how the capacity depends on the rank of this matrix. We will show how spreading out the antennas can result in near-full rank channel matrices (i.e. with close to n significant (non-negligible) eigenvalues), with corresponding high capacity, even in a purely LOS scenario without any scatterers. This work is based on [3].

This paper is organized as follows: In section II, we review the capacity expressions, and show explicitly the relationship between capacity and the rank of the channel matrix. In section III, we find the capacity for a Ricean channel matrix with various k -factors (power ratios between deterministic and scattered components), where the deterministic component is either of rank 1 or rank n . In section IV, we consider geometric ray tracing in a purely LOS environment, and show how the capacity increases as the spacing or angular spread between the n antenna elements is increased. In section V, we consider a specified environment (LOS down an urban street with building and ground reflections), with an n -element array with half-wavelength spacing, and show how the channel matrix approaches near-full rank (and the capacity increases) as the number of reflections considered is increased from zero to five. We also consider LOS scenarios with the base station array spread around the cell boundary, radiating inward. Section VI contains a summary and conclusions.

II. CAPACITY EXPRESSIONS

Next we will present some capacity expressions. We stress that the expressions are for a single communication link in a single cell with no adjacent channel interference. While capacity studies in a multi-user context, are of great

importance [4], they are beyond the scope of this paper.

We will be using T and R as convenient abbreviations for transmit and receive respectively. For example, in the next paragraph, we do this to subscript n to enumerate the number of antenna elements at a T site and R site respectively.

A. Basic Capacity expression

The fundamental result for the capacity in bps/Hz of a wireless system with n_T transmit antennas and n_R receive antennas with an average received SNR ρ (independent of n_T) at each receive antenna was obtained in [1] as

$$C = \log_2(\det[I_{n_R} + (\rho/n_T)HH^\dagger]) \quad (1)$$

where the normalized channel matrix H contains complex scalars with unity average power loss, and H^\dagger is the complex conjugate transpose of H . The capacity is expressed in bps/Hz in the narrowband limit with no frequency dependence. Normalization is achieved by dividing out the free space power loss and setting the parameter ρ to the desired SNR ². This result assumes that H is unknown to the receiver but n_R and ρ are known [1][2]. The signal from each antenna is different. The transmitted data has been demultiplexed and the demultiplexed substreams are separately independently coded and modulated. Moreover, instead of just committing the resulting subsignals one-to-one to the n_T transmit antennas, the association between substreams and antenna elements is cycled to encourage that over time each substream experiences a similar propagation environment.

If the matrix elements H_{ij} are random variables (e.g. Rayleigh, Ricean), then C is also a random variable. In this case, we define an outage threshold x (say 0.01), and define C_x to be that capacity for which $Prob\{C > C_x\} = 1 - x$.

B. Line-of-sight systems with closely spaced antenna elements

We consider an environment with only LOS propagation and T and R arrays of $n_T = n_R = n$ closely spaced antennas. Here we designate the base and subscriber ends of the link as T and R , respectively, but reciprocity applies, and all subsequent results apply to both the downlink (base-to-subscriber) and the uplink (subscriber-to-base). The T and R arrays are far apart relative to the array size. For this case, all the matrix elements have essentially the same amplitude and phases such that that $H = H_1$ (rank 1), as shown in the Appendix. An evaluation of HH^\dagger reveals all elements essentially equal to n , so that using the normalized H_1 , the matrix

$$A = [I_n + (\rho/n)HH^\dagger] \quad (2)$$

has all diagonal elements equal to $1 + \rho$, and all off-diagonal elements equal to ρ , so that $\det A = 1 + n\rho$. Thus for this case

$$C = \log_2(1 + n\rho) = C_{log} \quad (3)$$

²This avoids the need to compute absolute propagation loss and then set the transmitted power to obtain the desired SNR.

i.e. C_{log} increases logarithmically with n . For n closely spaced antennas, the capacity gain is essentially due to the n -fold gain in ρ .

C. Line-of-sight systems with widely spaced antenna elements

In general, with arrays of n more widely spaced antennas at T and R for which the path lengths between any pair of transmit and receive antennas are approximately the same to within the array size, the complex scalars H_{ik} all have magnitude 1 but different phases θ_{ik} . For such H , is it possible to obtain capacity exhibiting linear growth with n ? In this subsection we show, by mathematical example, that the answer is yes.

By choosing the θ_{ik} so that $HH^\dagger = nI_n$ in (2), all diagonal elements of A are $1 + \rho$, resulting in $\det A = (1 + \rho)^n$ and therefore

$$C = n \log_2(1 + \rho) = C_{lin} \quad (4)$$

i.e. C_{lin} increases linearly with n .

For a mathematical example of this particular type of H (denoted H_n) for which $HH^\dagger = nI_n$, take the generic ik entry of H_n to be given by

$$H_{ik} = \exp(j\theta_{ik}) \quad \text{where } \theta_{ik} = \frac{\pi}{n}((i - i_0) - (k - k_0))^2. \quad (5)$$

For $n = 2$ and $i_0 = k_0 = 0$,

$$H_n = \begin{pmatrix} 1 & j \\ j & 1 \end{pmatrix}. \quad (6)$$

A second example for which $HH^\dagger = nI_n$ is

$$H_{ik} = \exp(j\theta_{ik}) \quad \text{where } \theta_{ik} = \frac{2\pi}{n}(i - i_0)(k - k_0). \quad (7)$$

For $n = 2$ and $i_0 = k_0 = 0$,

$$H_n = \begin{pmatrix} -1 & 1 \\ 1 & 1 \end{pmatrix}. \quad (8)$$

Both types of $H \simeq H_n$ can be attained in practice by an appropriate geometrical arrangement of the T and R arrays. The first example above is two 2-element broadside arrays of appropriate spacing and separation to yield a path length difference $\delta = d(T_1, R_1) - d(T_1, R_2) = \lambda/4$. The second example is a 2-element array with $\lambda/2$ spacing at T with R comprising 2 elements equidistant from T , one broadside to T and one aligned (endfire) with T . The question of how widely spaced the antennas need to be to promote H tending to H_n is considered in section IV along with an investigation of robustness.

D. Rayleigh fading

For the case where we use a Rayleigh channel model so that the elements of H are random variables, we define $H_{Rayleigh}$ as a matrix of normalized (unit magnitude) uncorrelated complex gaussian variates. If $H = H_{Rayleigh}$,

then from [2], in the limit of large n and large ρ , the capacity lower bound approaches

$$C = n \log_2(\rho/e) \quad (9)$$

where $e = 2.718\dots$. This is close to the maximum capacity obtained with $H = H_n$. This result implies that there is a high probability that a particular realization of $H_{Rayleigh}$ has close to n significant (non-negligible) eigenvalues. This is as expected, since in the Rayleigh model $H_{Rayleigh}$ using *independent* complex gaussian variates, it is implicit that signals arrive from many directions³ i.e. the apparent transmitter locations are widely spaced.

III. CAPACITY ON RICEAN CHANNELS

Next consider the capacity for Ricean channels, where the deterministic (e.g. LOS) component H_{LOS} is fixed as either H_1 or H_n . We follow the simulation methods of [1] using the normalized Ricean channel matrix

$$H = (aH_{LOS} + bH_{Rayleigh}) \quad (10)$$

with $a^2 + b^2 = 1$. The Ricean k -factor, $k = a^2/b^2$, is the ratio of the LOS power to the scattered power, and varies from 0 (pure Rayleigh) to ∞ (pure deterministic).

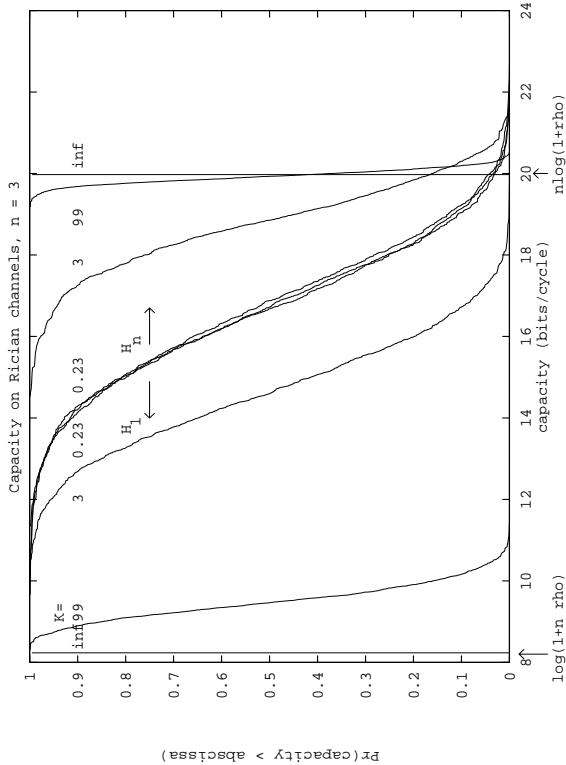
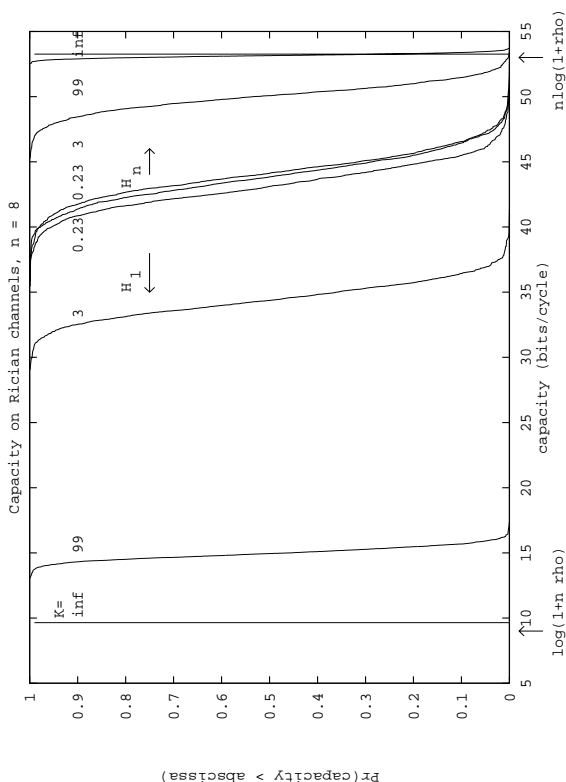
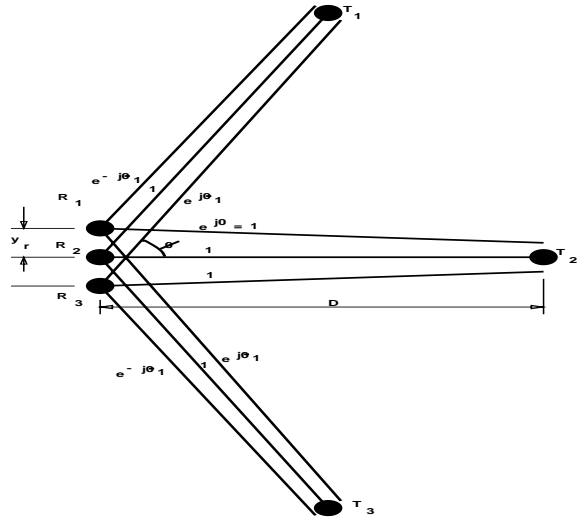
The results for $n = 3$ and 8 with $\rho = 100$ (20 dB) (Figures 1,2) quantify how for $H_{LOS} = H_1$, the capacity decreases with increasing k , and, in the limit of $k = \infty$, $C = C_{log}$. However, for $H_{LOS} = H_n$, the capacity increases with increasing k , and in the limit of $k = \infty$, $C = C_{lin}$. An expanded scale plot for $n = 8$ shows that the $k = 0$ case capacity tends towards $n \log_2(\rho/e)$.

IV. MAXIMUM LOS CAPACITY

To find the maximum capacity which may be realized in practice in a LOS environment, we seek to construct geometric arrangements of the T and R arrays such that $H_{LOS} \simeq H_n$. Again, we designate the base and subscriber ends of the link as T and R , respectively, but reciprocity applies, and all subsequent results apply to both the downlink (base-to-subscriber) and the uplink (subscriber-to-base). Specifically, we ask what antenna spacing at T and R is required to obtain the θ_{ik} in H_n , and what spacing at T is required if the spacing at R is constrained to a half-wavelength. For these spacings, $H_{LOS} \simeq H_n$ as a direct result of ray-tracing calculations for the chosen geometry. We stress that the transmitter does not use detailed channel knowledge in any way. We are maintaining our assumption that each of the n antennas carries a separate component of the information and that the transmitter does not know the channel and does not adjust the power or phase of the n information components to fit the channel.

To achieve $C \simeq C_{lin}$, the H_{ik} need not be exactly according to (5)(7). Numerical results show that $C \simeq C_{lin}$ even if the off-diagonal elements in HH^\dagger are non-zero with values up to $n/3$. Thus the capacity is robust in the presence of

³For a given interelement spacing at R , see [8] for the angular spread of signals from T required in order to achieve zero correlation between R elements.

Fig. 1. Capacities of Ricean channels, $n=3$.Fig. 2. Capacities of Ricean channels, $n=8$.Fig. 3. Transmit and receive arrays, small spacing at R

small variations in the geometric arrangements, as will be observed in Section V.

A. R array constrained to practical size

We consider a 3-element transmit and receive array (Figure 3), where the R array is constrained to have a fixed small interelement spacing y_r (e.g. $y_r = \lambda/2$), so that the size of R is practical. We seek to find the interelement spacing of T for which capacity is maximum. To preserve the property that all elements of H have unit magnitude, all rays from T to R must be approximately the same length, and thus the T array is in the shape of an arc. We will assume that the T - R distance $D \gg y_a = y_r(n-1)$, where y_a is the size of the linear R array, so that we can assume plane wave arrivals from each element of T across the entire array R . Thus the T interelement spacing is defined by the angle ϕ between T array elements as seen at R , and ϕ will be independent of D .

The geometrical symmetry allows us to write the normalized matrix channel

$$H_{LOS} = \begin{pmatrix} e^{-j\theta_1} & 1 & e^{j\theta_1} \\ 1 & 1 & 1 \\ e^{j\theta_1} & 1 & e^{-j\theta_1} \end{pmatrix} \quad (11)$$

For this particular case, H_{LOS} is in the form (7) with $i_0 = k_0 = 2$, and solving for θ_1 such that $H_{LOS} = H_n$ (i.e. $HH^\dagger = nI_n$) yields $\theta_1 = 120$ degrees, with corresponding path length difference

$$\delta = d(T_1, R_1) - d(T_1, R_2) = \frac{120}{360} \lambda = \frac{\lambda}{3} \quad (12)$$

(Figure 3). From the geometry, $\delta = y_r \sin \phi$ or $\sin \phi = \frac{\delta}{y_r} = \frac{\lambda/3}{\lambda/2} = \frac{2}{3}$, so that the angular size of the arc $2\phi = 2\arcsin(2/3) = 84$ degrees. We can similarly construct $H_{LOS} \simeq H_n$ for arbitrary n , as shown in the Appendix.

The geometrical interpretation arising in the Appendix is that the radiation pattern of R with all elements in phase has nulls in the direction of all but the center element of T .

B. Discussion

In practice, the path lengths between different antennas pairs are not all the same, so that H_{LOS} is not precisely equal to H_n , and $C = C_{lin}$ is not quite attained. The ray tracing calculations in Section V are needed to obtain precise results for the capacity as a function of spacing y_r or the angular size of the arc 2ϕ .

We will find that for the R array constrained to half-wavelength spacing, the angular range of the arc of the T array increases slowly with n , reaching $2\phi = 108$ degrees for $n = 8$. The large n result⁴ is consistent with the angular spread of signals $2\Delta \simeq \frac{30}{y_r/\lambda}$ [8] required to obtain near zero correlation between array elements for $y_r = \lambda/2$, and thus is intuitively satisfying. This result remains consistent with other values of y_r . The formal relationship between [8] and the present work is considered in the Appendix by replacing the random sources (scatterers) located within the angular range 2Δ [8] with the n elements of T within the same angular range.

V. CAPACITY IN SPECIFIED ENVIRONMENT USING RAY TRACING

Capacities available in a specific environment were obtained in [5] using ray tracing for the case of a single transmit antenna ($n_T = 1$) and multiple receive antennas. In this section, we seek to extend this work for the case $n_T > 1$. A simple ray-tracing program which can accommodate some simple illustrative geometries was used. We will find H_{LOS} for various LOS geometries with no scatterers, as well as an urban street with 3 reflecting (scattering) surfaces, i.e. two walls (buildings) and the ground.

A. Geometry and coordinates

The urban street geometry contains two parallel reflectors representing the building walls, separated by the street width a . A top view is shown in Figure 4, where the ground is the y - z plane. The n array elements at each of T and R and the images I^k have coordinates $R_j : (x_{r_j}, y_{r_j}, z_{r_j})$, $T_i : (x_{t_i}, y_{t_i}, z_{t_i})$, $I_i^0 : (-x_{t_i}, y_{t_i}, z_{t_i})$, $I_i^{+1} : (x_{t_i}, 2a - y_{t_i}, z_{t_i})$, $I_i^{-1} : (x_{t_i}, -y_{t_i}, z_{t_i})$, with $i, j = 1, \dots, n$, where we define the reference location to be the first element $T_1 : (x_{t_1}, y_{t_1}, z_{t_1}) = (x_{t_1}, y_{t_1}, z_{t_1})$ and similarly for R . $I^{\pm k}$ represents an image due to k specular reflections from the walls, and I_i^0 is the ‘ground reflection’ image not visible in the figure. A general expression for the coordinates of I^k is given in [6]. In this first example, the T and R arrays are oriented perpendicular to the street direction, with half-wavelength antenna spacing, so that $x_{t_i} = x_t$, $y_{t_i} = y_t + i\lambda/2$, $z_{t_i} = z_t$, and $x_{r_j} = x_r$, $y_{r_j} = y_r + j\lambda/2$, $z_{r_j} = z_r$,

⁴If we define $2\phi = f(n-1)360/n$ to take care of end effects due to finite n (see the Appendix), then we find $f \simeq 1/\pi$ for all n . Thus in the limit of large n , the range of arc $2\Delta = (0.32)(360) = 120$ degrees

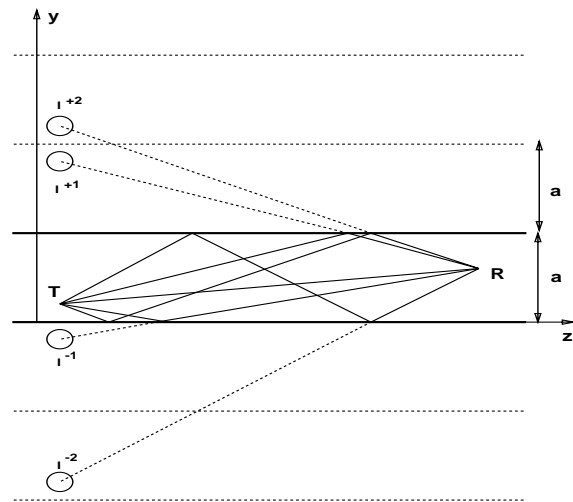


Fig. 4. Images in street canyon - top view

In the absence of any scattering surfaces, we have only the LOS path and $C \simeq C_{log}$ ⁵ However, with scattering surfaces present, we anticipate that the images may be sufficiently spread apart for C to approach C_{lin} . We make explicit calculations of C in the sequel.

For the street geometry outlined above, the elements of H may be written

$$\frac{H_{ij}}{|T_1 - R_1|} = \frac{\exp(-j2\pi|T_i - R_j|/\lambda)}{|T_i - R_j|} + \sum_{k=-m}^m \Gamma^k \frac{\exp(-j2\pi|I_i^k - R_j|/\lambda)}{|I_i^k - R_j|} \quad (13)$$

where Γ is the amplitude reflection coefficient⁶, m is the maximum number of reflections considered, and we have assumed isotropic antennas. H_{ij} is normalized by the distance between the reference locations T_1, R_1 , so that the absolute attenuation need not be calculated. Here we assume a fixed frequency $f = c/\lambda$.

B. Capacity results

We use the expressions for H_{ij} in the preceding sections to obtain numerical results for capacity in the specified geometries. For all these results, $\rho = 100$ (20 dB) at the reference distance D .

B.1 Street scenario

We consider the street scenario with the images added, and the two arrays oriented broadside to each other, each

⁵In fact, $C = C_{log}$ for zero spacing between elements, and C is slightly greater than C_{log} for half-wavelength spacing.

⁶In general, the Γ are different for each image, since they depend on the angles of incidence and reflection. Here we assume Γ has the same constant value for all reflections, except the ground reflection Γ^0 which is set to -1 . This approximation suffices to illustrate the capacity gain.

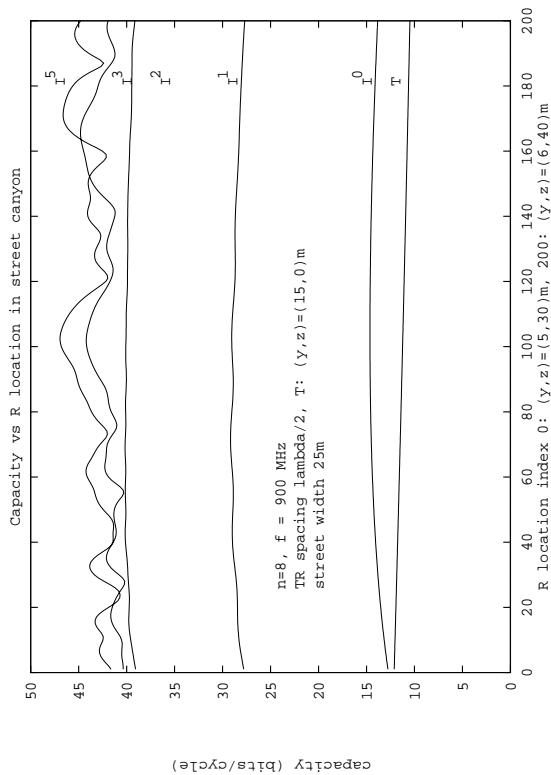


Fig. 5. Capacity versus R location in street canyon

with interelement spacing fixed at a half-wavelength. The parameters used are: wavelength $1/3$ meter, street width $a=25$ meters with walls at $y = 0$ and 25 , $(x_t, y_t, z_t) = (10, 15, 0)$, $(x_r, y_r, z_r) = (1, 5, 30)$, all dimensions in meters. Γ is set to 0.6 , so that the average total power received from reflections only, with 5 reflections, is equal to the average LOS power. The ground reflection coefficient is set to -1 . Figure 5 shows the capacity as a function of (x_r, y_r, z_r) ranging in 200 steps from $(1, 5, 30)$ to $(1, 6, 40)$ meters (about 30 wavelengths). The capacity increases as more images are added, and matches the 90 percent Rayleigh capacity obtained in Figure 2 for $n = 8$ with 7 images ($k = 0, \dots, \pm 3$ in eqn. (13)) plus T . Furthermore, the received signal envelope looks increasingly Rayleigh-like as more images are added. The power increase resulting from adding images accounts for some, but not all of the capacity increase.

These results show that capacity can be increased by spreading out the elements of the T array (implicitly) by creating images of the (closely-spaced) T array. Thus we effectively have an $m \times n$ element T array, where $m - 1$ is the number of images, and n distinct signals are each simulcast m times. The implicit spreading of the T array may be achieved in an urban scenario by lowering the array below the rooftops⁷.

⁷This idea of lowering the transmit antennas below the rooftops was first suggested by M. J. Gans.

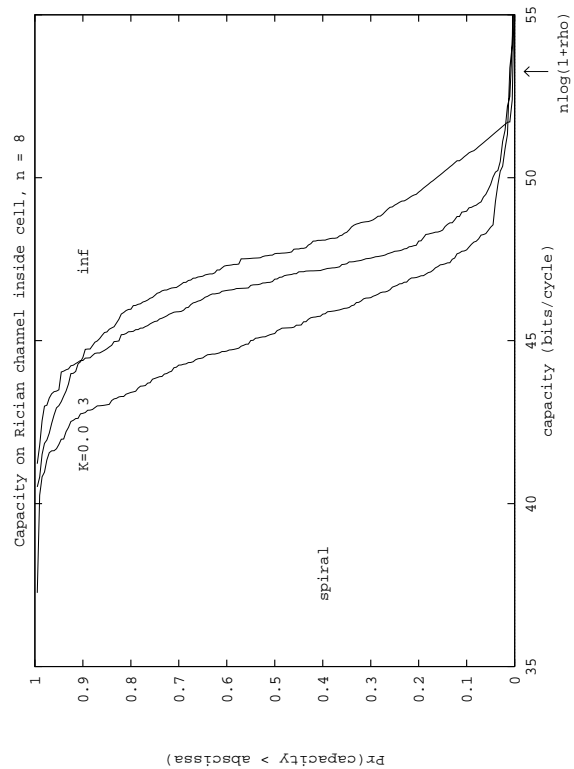


Fig. 6. Capacity on Rician channel inside cell, $n=8$, $\rho = 20$ dB at center

B.2 T array in circle along cell boundary

We further investigate the idea of explicitly spreading out the T array by considering n elements in a circle of radius $D_t = 10,000\lambda = 3,333\text{m}$ for $\lambda = 1/3$ m ($f = 900$ MHz), with R comprising n elements on a circle with radius $D_r = \lambda/2 = 0.16$ m⁸. For this case, $x_{r_j} = x_r, y_{r_j} = y_r + D_r \cos[\frac{2\pi}{n}(j + 0.5)]$, $z_{r_j} = z_r + D_r \sin[\frac{2\pi}{n}(j + 0.5)]$, and similarly for T .

Figure 6 shows the probability distribution of capacity for 200 points uniformly distributed within the cell for various Rician k -factors, where the total signal power is determined by the R location within the cell. The large circular T array replicates the implicit assumption in Section III that H_{Rayleigh} is the result of equal power signals arriving from many directions. The result for $k = 0$ corresponds to that in Figure 2. The larger k -factors improves the capacity beyond that obtained with a pure Rayleigh channel matrix.

B.3 T array in partial circle

We investigate the capacity as a function of the angular spread of the arriving signals by reducing the T array from a full circle to an arc. Thus $x_{t_i} = x_t, y_{t_i} = y_t + D_t \cos[f\frac{2\pi}{n}(i - \frac{n-1}{2})]$, $z_{t_i} = z_t + D_t \sin[f\frac{2\pi}{n}(i - \frac{n-1}{2})]$, where f is the fraction of the full 360 degree arc. We also replace the circular R array with a λ or $\lambda/2$ spaced linear array oriented along the z -axis broadside to the center of

⁸The results are not sensitive to the value of $D_t \gg \lambda$.

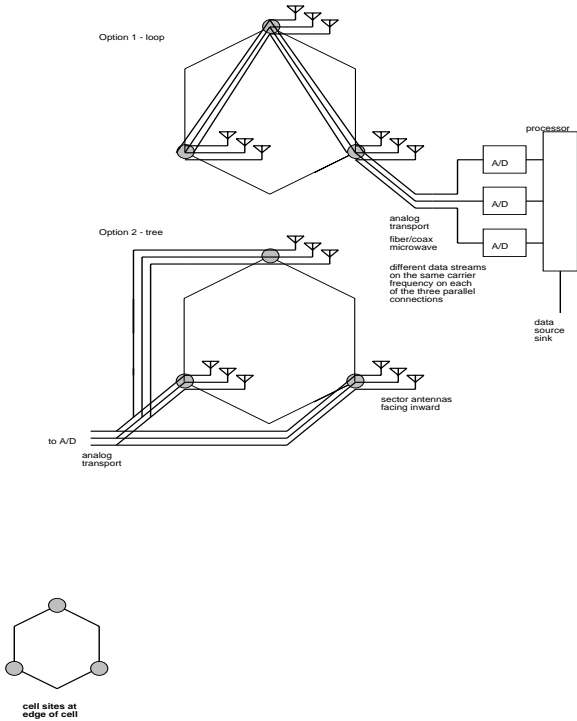


Fig. 7. Inward-facing (edge-excited) cell

the arc.⁹ for $y_r = \lambda$ and $y_r = \lambda/2$ respectively¹⁰. Maximum capacity C_{lin} is achieved for $f \simeq 0.35$ for $\lambda/2$ spacing, and is independent of D_t provided that ρ is set to 20 dB for R at the center of the arc. The same value of f was found for all n in the range 3-8. Thus in the limit of large n , the range of arc $2\phi = (0.35)(360) = 126$ degrees for $\lambda/2$ spacing at R , which is consistent with the results of [8], as previously mentioned in Section IV. Similarly, the results for λ spacing were consistent. In the Appendix, we note that maximum capacity is attained when the locations of the n array elements of T corresponds closely with the nulls in the radiation pattern of R . This result is robust and can be attained in practice, since the off-diagonal elements in HH^\dagger can be non-zero, as mentioned Section IV and in the Appendix.

The capacity with a circular (instead of linear) array of radius $\lambda/2$ at R increases monotonically with f , and achieves C_{lin} only for $f \simeq 1$.

VI. SUMMARY AND CONCLUSIONS

Wireless communications systems with multiple antennas at both transmitter and receiver have an information-theoretic channel capacity which can grow linearly (rather than logarithmically) with the number of antennas [1] for fixed total radiated power and fixed bandwidth. This result assumes that the transmitter does not know the channel,

⁹The angular spread of the two end elements of T is $2\phi = f(n-1)360/n$ because of end effects due to finite n , see also the Appendix.

¹⁰Again, we use $D_t = 10,000\lambda = 3,333$ meters, but the results are not sensitive to the value of $D_t \gg \lambda$.

and that separate information is sent out of each transmitter antenna. Here we show that such capacities can be achieved not only on Rayleigh channels with many scatterers, but also on deterministic channels with direct LOS paths only and no scatterers, by explicitly spreading out the antennas well beyond a wavelength. This has significant implications for application areas such as indoor wireless LANs.

Capacities approaching $C_{lin} = n \log_2(1 + \rho)$ can be achieved in a deterministic LOS (non-Rayleigh) environment. This is achieved by spreading the elements of T either explicitly (by placing one element of T at each of n sites), or implicitly (by adding reflectors which create images of T). This result suggests that in the absence of reflectors, the T array can be explicitly spread apart, but using n antennas instead of one at each of n sites, thus duplicating the effect of images (Figure 7). The models for $H = H_{LOS} + H_{Rayleigh}$ described here may be useful for the testing of wireless systems which exploit the available capacity (e.g.[2]).

The results for a linear array at R may be interpreted physically in two ways. First, capacities approaching C_{lin} are attained in a deterministic environment by spreading the n array elements of T evenly around an arc with the same angular range required to obtain zero correlation between R elements in a scattering environment [8]. Thus the continuum of sources (scatterers) along the arc assumed in [8] is replaced by n discrete elements of T spread out over the same angular range. Second, C_{lin} is precisely attained when the locations of the T array elements along the arc corresponds precisely with the nulls in the radiation pattern of R , i.e. they are spaced almost, but not quite, evenly around the arc, assuming equal phase at all T elements. However, the spacing need not be so precise to attain capacities close to C_{lin} . For given spacing at R , increasing n results in more closely spaced nulls, and the angular range of the n array elements of T does not change. In both interpretations, the angular range of the arc depends only on the spacing of the R elements, and is independent of n .

We conclude that high capacities may be achieved in several ways: 1) The transmit antenna array can be spread out. The interelement spacing or angular spread may be such that n separate base station sites are needed [11]. However, capacity may be lost if some of the base station sites are shadowed from the mobile. 2a) The n antennas at a single base site are implicitly duplicated by placing them in a scattering environment where images are created. This may be viewed as a kind of implicit spreading of the transmit array. 2b) The n antennas are duplicated at each of the n base sites, to minimize shadowing loss (n -conductor leaky feeder with n leaks, thus using n^2 radiators for n -times simulcasting of the n signals). This scheme may be viewed as explicitly creating images (duplicates) where there are no scatterers to create them implicitly. 2c) A preferred arrangement for 2b is a leaky feeder arrangement with the n leaks around the cell boundary facing inward. This arrangement yields constant high capacity near C_{lin} within the cell coverage area.

In summary, to maximize the number of degrees of freedom to enhance capacity, the transmitter array is spread out explicitly/implicitly in the absence/presence of scatterers.

VII. ACKNOWLEDGMENTS

The author thanks G.J. Foschini for our delightful collaboration on [3], and L.J. Greenstein for ideas and support during visits to AT&T.

APPENDIX

I. GENERAL FORMS OF H_{LOS} AND HH^\dagger

A. R linear, T arc

We consider an n element T array spread evenly along an arc, and a linear R array oriented broadside to the center of the arc (Figure 2). The angles of arrival of the ray path at R from the l th element of T ($l = 0, \dots, n-1$) may be written

$$\phi_l = f \frac{2\pi}{n} \left(l - \frac{n-1}{2} \right) \quad (14)$$

where f is the fraction of the full 360 degree arc subtended by the elements of T (section V B). The angular spread between the first and last element of T is $2\Delta = \phi_{n-1} - \phi_0 = 2\pi f \frac{n-1}{n}$. The radius of the arc $D_t \gg \lambda$, so that plane waves arrive at R .

For this geometry, the normalized ik element of H_{LOS} may be written

$$H_{ik} = \exp \left(j \frac{2\pi z_r}{\lambda} \left[(i-1) - \frac{n-1}{2} \right] \sin \phi_{k-1} \right) \quad (15)$$

for $i, k = 1, \dots, n$. z_r is the interelement spacing, and the center of the R array is assumed to have zero phase¹¹. The ik element of HH^\dagger is thus

$$(HH^\dagger)_{ik} = \sum_{l=0}^{n-1} \exp \left(j \frac{2\pi z_r}{\lambda} (i-k) \sin \phi_l \right) \quad (16)$$

For $z_r = \lambda/2$, $C \simeq C_{lin}$ for $f \simeq 0.35$ for $n = 3, \dots, 8$ ¹² corresponding to an angular spread $2\Delta \simeq 2\pi f = 126$ degrees. This is consistent with the beamwidth $\Delta \simeq \frac{30}{z_r/\lambda} = 60$ degrees at which zero correlation is obtained [8]. We note that (16) corresponds to the autocorrelation $R_{xx}(i-k) = \frac{1}{2\Delta} \text{Re} \int_{-\Delta}^{\Delta} e^{j \frac{2\pi z_r}{\lambda} (i-k) \sin \beta} d\beta$ from [8] equation (A-13)¹³, specialized for n discrete angles of arrival ϕ_l .

The radiation pattern of the array with all elements in phase $E(\phi) = \frac{\sin(n\gamma/2)}{n \sin(\gamma/2)}$ where $\gamma = 2\pi z_r \sin \phi / \lambda$, $z_r = \lambda/2$ has nulls at $\phi = \arcsin \phi_l$ for odd n and $f = 1/\pi$. Thus the array elements of T would be precisely in the nulls of R by changing their spacing slightly. Thus we substitute $\phi_l \simeq \arcsin \phi_l = \arcsin \frac{2}{n} \left(l - \frac{n-1}{2} \right)$, in (15) to obtain

$$H_{ik} = \exp \left(j\pi \left[(i-1) - \frac{n-1}{2} \right] \frac{2}{n} \left[(k-1) - \frac{n-1}{2} \right] \right) \quad (17)$$

¹¹In general, the zero phase point may be set anywhere along the R array, resulting in a shift in the i index.

¹²However HH^\dagger is not precisely equal to nI except for $n = 3$.

¹³The sum (16) is real

which is in the form (7), so that $HH^\dagger = nI_n$.

B. R, T both full circular arrays

We consider an n element T array with elements spread evenly around a circle of radius $D_t \gg \lambda$, and a similar R array on a circle of radius $D_r \leq \lambda$ at the center of the T array. For this case, the normalized ik element of H_{LOS} may be written

$$H_{ik} = \exp \left(j \frac{2\pi D_r}{\lambda} \cos \left[(i-k) \frac{2\pi}{n} \right] \right) \quad (18)$$

The ik element of HH^\dagger is thus

$$(HH^\dagger)_{ik} = \sum_{l=0}^{n-1} \exp \left(j \frac{2\pi D_r}{\lambda} \cos \left[(i-l) \frac{2\pi}{n} \right] \right) \cdot \exp \left(-j \frac{2\pi D_r}{\lambda} \cos \left[(k-l) \frac{2\pi}{n} \right] \right) \quad (19)$$

with diagonal elements equal to n . For $D_r = \lambda/2$, the elements of HH^\dagger for which $i-k$ is odd are zero, but the even elements are approximately $0.3n$ for $n = 8$. Nonetheless, the capacity approaches C_{lin} , consistent with the observation [8] that small correlation (< 0.3) has negligible effect on performance.

REFERENCES

- [1] G.J.Foschini, M.J. Gans, 'On limits of wireless communication in a fading environment when using multiple antennas', *Wireless Personal Communications*, vol. 6, no.3, pp.311-335, Mar. 1998.
- [2] G.J.Foschini, 'Layered space-time architecture for wireless communication in a fading environment when using multi-element antennas', *Bell Labs Technical Journal*, vol. 2, no. 2, pp. 41-59, Autumn 1996.
- [3] P.F. Driessen, G.J. Foschini, 'On the capacity of multiple-input multiple-output wireless channels: a geometric interpretation', *IEEE Trans. Commun.*, vol. 47, no.2, pp. 173-176, Feb. 1999.
- [4] S. Catreux, P.F. Driessen, L.J. Greenstein, 'Simulation results for an interference-limited multiple-input multiple-output cellular system', *IEEE Communications Letters*, June 2000.
- [5] G.J.Foschini, R.A. Valenzuela, 'Initial estimation of communication efficiency of indoor wireless channels', *International Journal of Wireless Information Networks*, 1996.
- [6] P.F. Driessen et al, 'Ray model of indoor propagation' in T. Rappaport, M. Feuerstein, *Personal Communications Networks*, Kluwer Academic Press, 1992.
- [7] P.Beckmann, A.Spizzichino, *The scattering of electromagnetic waves from rough surfaces*, Permagon, 1963.
- [8] J.Salz, J.H.Winters, "Effect of fading correlation on adaptive arrays in digital mobile radio", *IEEE Trans. Vehic. Tech.*, vol. 43, no. 4, pp. 1049-1057, November 1994.
- [9] S. Ariyavisitakul, T. E. Darcie, L. J. Greenstein, M. R. Phillips and N. K. Shankaranarayanan 'Performance of simulcast wireless techniques for Personal Communication Systems', *IEEE Sel. Areas Commun.*, Vol. 14, No. 4, May 1996, pp. 632-643.
- [10] F. Borgonovo, A. Acampora, 'Capture division multiple access: a new cellular access architecture for future PCN's', *IEEE Comm. Mag.*, Vol.34, No.9, September 1996, p. 154-162.
- [11] P.F. Driessen, 'Cellular communication system with multiple same frequency broadcasts in a cell', *US Patent 6,052,599*, April 2000.